Organic and Biomolecular Chemistry

ARTICLE

Self-assembly of Ni-NTA-modified β-Annulus Peptides into Artificial Viral Capsids and Encapsulation of His-tagged Proteins

Received 00th January 20xx,
Accepted 00th January 20xx

DOI: 10.1039/x0xx00000x

www.rsc.org/

Kazunori Matsuura,*[a] Tomohiro Nakamura,[b] Kenta Watanabe,[b] Takanori Noguchi,[b] Kosuke Minamihata,[b] Noriho Kamiya,[b,c] and Nobuo Kimizuka[b,d]

β-Annulus peptide bearing Cys at the N-terminal from tomato bushy stunt virus was synthesised using a standard Fmoc-protected solid-phase method, and the petide was modified with Ni-NTA at the N-terminal. The Ni-NTA-modified β-annulus peptide self-assembled into virus-like nanocapsules of approximately 40 nm in diameter. The critical aggregation concentration of these nanocapsules in 10 mM Tris-HCl buffer (pH 7.3) at 25°C was 0.053 μM, which is 470 times lower than that of unmodified β-annulus peptides. Moreover, size exclusion chromatography of the peptide assembly indicated encapsulation of His-tagged green fluorescent protein in the Ni-NTA-modified artificial viral capsid.

Introduction

Viral capsids with rod-like or spherical morphology are exemplary natural supramolecular assemblies with discrete aggregation numbers and have been used as nanocontainers for inorganic materials, drugs and proteins.[1] In particular, the encapsulation of proteins into spherical viral capsids has potential for developing novel drug delivery systems and enzymatic nanoreactors.[2-4] Accordingly, Cornelissen and co-workers encapsulated horse radish peroxidase and green fluorescence protein (GFP) into the recombinant cowpea chlorotic mottle virus (CCMV) capsid.[2] Moreover, Hilvert and co-workers reported regarding the encapsulation of GFP into the virus-like capsid of lumazine synthase from Aquifex aeolicus.[4]

Chemical strategies for rational designs of artificial peptide and protein assemblies have been progressively developed for constructing virus-like nanoarchitechtures.[5-10] Specifically, Yeates and co-workers constructed discrete protein nanocages by self-assembly of fusion proteins possessing dimer- and trimer-forming subunits.[7] Woolfson and co-workers also succeeded in constructing unilamellar spheres of approximately 100-nm size by self-assembly of two complementary coiled-coil hubs.[8] We previously demonstrated that artificial C_3-symmetric peptide conjugates self-assemble into virus-like nanospheres.[11-13] However, it was difficult to encapsulate guest macromolecules into these nanospheres comprising of designed proteins or peptides because of the lack in methodology to selectively functionalize interior of the nanospheres.

We recently demonstrated that the designed 24-mer β-annulus peptide fragment INHVGGTGGAIMAPVAVTRQLVGS, which is found as a protein motif in tomato bushy stunt virus capsids, self-assembled into virus-like nanocapsules (artificial viral capsid) of 30–50 nm.[14] The pH dependence of the ζ-potential of artificial viral capsids suggests that the C-terminals of peptides are directed toward the outer surface while the N-terminals are directed towards the interior.[14b] These properties enabled selective modification of artificial viral capsids surface with gold nanoparticles by C-terminal modification of the β-annulus peptide.[14d] In contrast, the N-terminal-directed interior of nanocapsules might be cationic at neutral pH, enabling the encapsulation of DNA[14b] and anionic quantum dots[14f] inside the artificial viral capsids. In this study, we designed a novel β-annulus peptide modified with Ni-NTA (nitrilotriacetic acid) **1** at the N-terminal. Subsequently, we demonstrated the construction of an artificial viral capsid with internal Ni-NTA and showed its interaction with His-tagged GFP (Figure 1).

Results and discussion

A β-annulus peptide bearing Cys at the N-terminal **2** (CINHVGGTGGAIMAPVA VTRQLVGS) was synthesised using a standard Fmoc-protected solid-phase method. Cys of peptide 2 was reacted with maleimido-C_3-NTA to obtain NTA-modified β-annulus peptides. After purification using reverse-phase HPLC, Ni-NTA-modified β-annulus peptide **1** was prepared by mixing with equimolar $NiCl_2$, and the identity of the peptide was confirmed using MALDI-TOF-MS (m/z = 2892.3 $[M + H]^+$).

[a] Department of Chemistry and Biotechnology, Graduate School of Engineering, Tottori University, Tottori 680-8552, Japan. E-mail: ma2ra-k@chem.tottori-u.ac.jp.
[b] Department of Applied Chemistry, Graduate School of Engineering, Kyushu University, Fukuoka 819-0395, Japan.
[c] Division of Biotechnology, Center for Future Chemistry, Kyushu University, Fukuoka 819-0395, Japan.
[d] Center for Molecular Systems (CMS), Kyushu University, Fukuoka 819-0395, Japan.

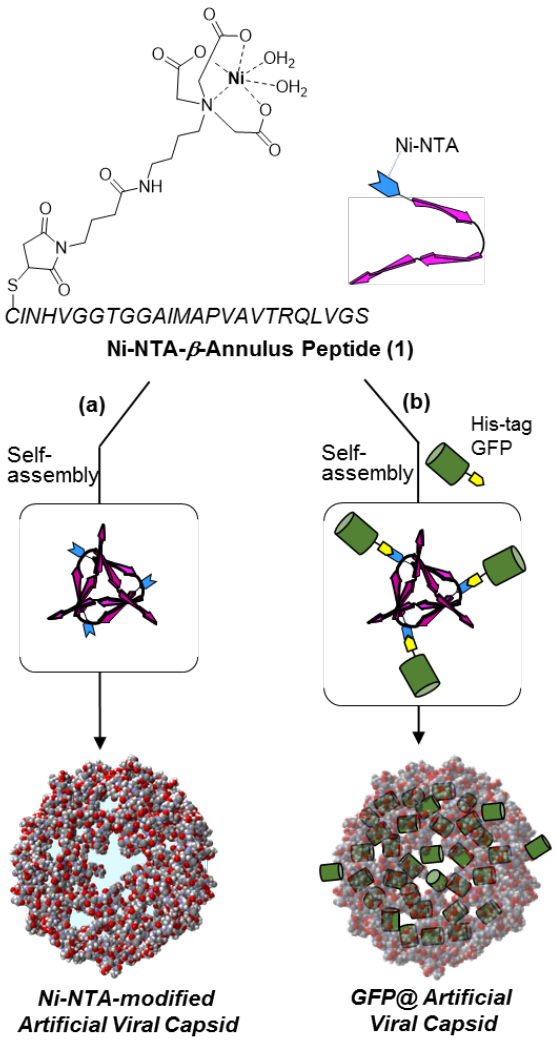

Fig. 1 Schematic of (a) the formation of Ni-NTA-modified artificial viral capsids by self-assembly of Ni-NTA-modified β-annulus peptide **1**, and (b) complexation of His-tagged EGFP with Ni-NTA-modified synthetic viral capsid.

Self-assembly of Ni-NTA-modified β-annulus peptide **1** in 10 mM Tris-HCl buffer (pH 7.3) was investigated using scanning electron microscopy (SEM), transmission electron microscopy (TEM), and dynamic light scattering (DLS). In SEM images, spherical assemblies of 25–40-nm diameters were abundantly observed (Figure 2A). TEM images stained with phosphotungstic acid also showed spherical assemblies of about 40-nm diameters (Figure 2B). The black centres of the structures in the TEM images might be caused by an accumulation of phosphotungstic acid in the interior of the spherical assemblies. Moreover, DLS analyses revealed average hydrodynamic diameters of 46.8 ± 10.5 nm (Figure 2C), which is comparable to the diameter of artificial viral capsids that self-assembled from unmodified 24-mer β-annulus peptide **3** (INHVGGTGGAIMAPVAVTRQLVGS).[14a] Therefore, modification of the β-annulus peptide with Ni-NTA at the N-terminal minimally affected sizes and morphologies of the resulting capsids. The concentration dependence of Ni-NTA-modified β-annulus peptide **3** scattering intensities indicates

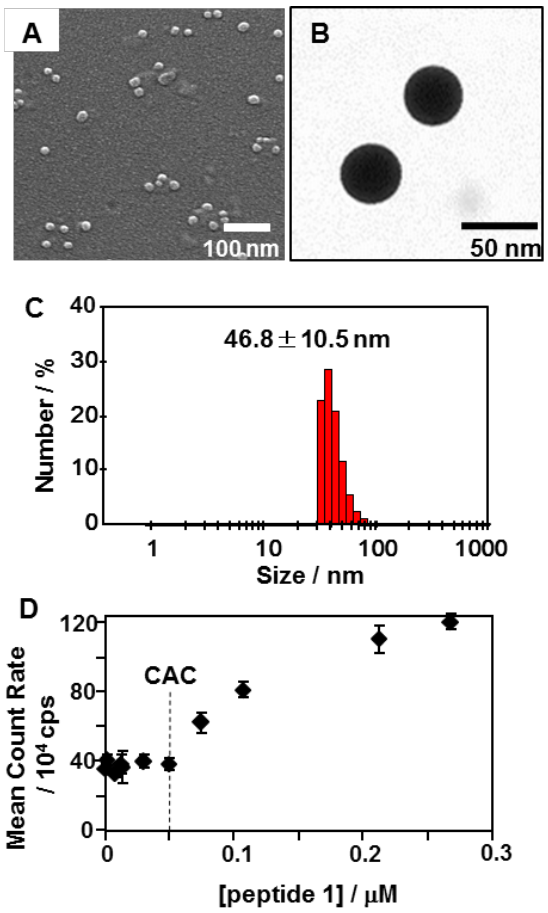

Fig. 2 (A) SEM and (B) TEM images of aqueous solutions containing Ni-NTA-modified β-annulus peptide **1** (0.1 mM) in 10 mM Tris-HCl buffer (pH 7.3) at 25°C. The SEM sample was coated with 3 nm Pt. The TEM sample was stained with 2% phosphotungstic acid. (C) Size distributions from dynamic light scattering (DLS) analyses of the aqueous solution. (D) Effects of Ni-NTA-modified β-annulus peptide **1** concentrations on the scattering intensity obtained from DLS in 10 mM Tris-HCl buffer (pH 7.3) at 25°C.

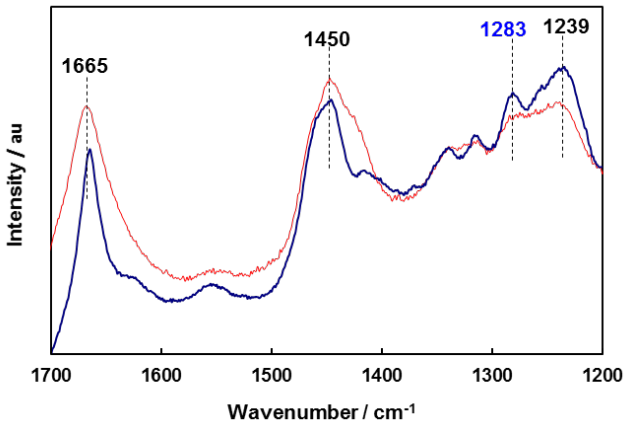

Fig. 3 Raman spectra of NTA-modified β-annulus peptide (red) and Ni-NTA-modified β-annulus peptide **1** (blue) on silicon wafer (excitation wavelength: 532 nm).

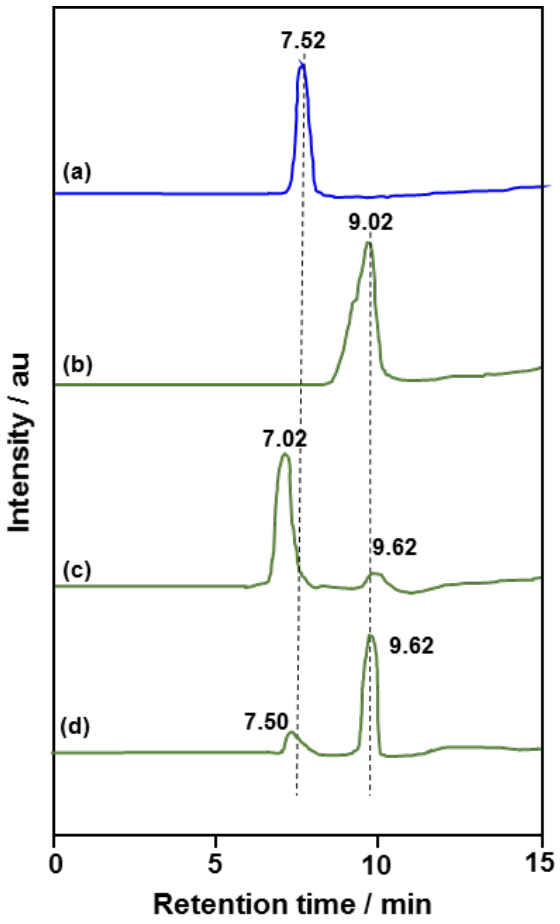

Fig. 4 Size exclusion chromatograph of (a) assemblies of Ni-NTA-modified *β*-annulus peptide **1** (detected at 220 nm); (b) His-tagged EGFP alone was detected at 488 nm; (c) Equimolar mixtures of His-tagged EGFP and Ni-NTA-modified *β*-annulus peptide **1** assemblies were detected at 488 nm; (d) Equimolar mixtures of His-tagged EGFP and assemblies of unmodified *β*-annulus peptide 3 were detected at 488 nm.

that the critical aggregation concentration (CAC) in 10 mM Tris-HCl buffer (pH 7.3) at 25°C is 0.053 μM (Figure 2D), whereas that of unmodified *β*-annulus peptide **3** under the same conditions was 25 μM.[14a,f] These remarkable differences in CACs suggest that the artificial viral capsid that was self-assembled from Ni-NTA-modified β-annulus peptide **1** was more stable than that from unmodified *β*-annulus peptide **3**. Hence, artificial viral capsids comprising peptide **1** are seemingly stabilised by electrostatic interactions between negative charges of the Ni-NTA complex and N-terminal ammonium ions. In addition, Raman spectrum of the artificial viral capsids comprising peptide **1** showed a peak at 1283 cm^{-1} that was assigned to Ni–His coordination (Figure 3),[15] suggesting stabilization of artificial viral capsids by crosslinking of Ni-NTA with His residues of different peptide chain.

Size exclusion chromatography (SEC) of Ni-NTA-modified *β*-annulus peptide **1** assemblies showed a single elution peak at 7.52 min (Figure 4a), reflecting enhanced stability of the

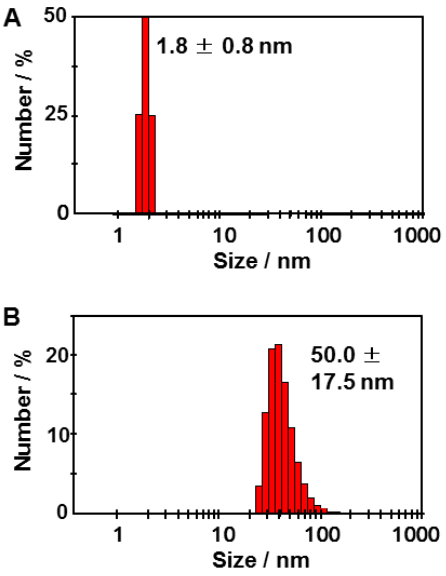

Fig. 5 Size distributions from DLS experiments with aqueous solutions of (A) His-tagged EGFP alone and (B) equimolar mixtures of His-tagged EGFP and peptide **1** assemblies in 10 mM Tris-HCl buffer (pH 7.3) at 25°C; [His-tagged EGFP] = [**1**] = 0.1 mM.

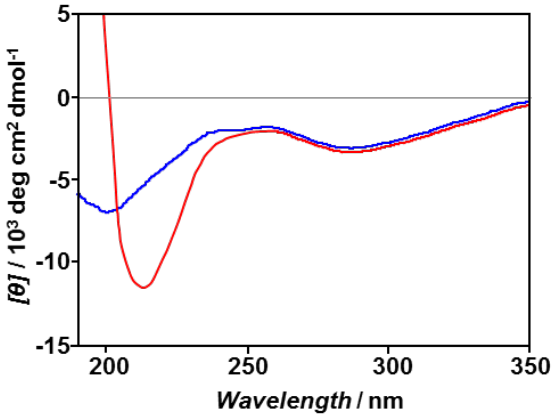

Fig. 6 CD spectra of peptide **1** assemblies in the absence (blue) and presence (red) of His-tagged EGFP of in 10 mM Tris-HCl buffer (pH 7.3) at 25°C; [His-tagged EGFP] = [**1**] = 0.1 mM.

artificial viral capsid. The apparent number average molecular weight of Ni-NTA-modified *β*-annulus peptide **1** assemblies was estimated as 185 kDa using calibration curve of protein standards (see Experimental section). The apparent aggregation number was then calculated by dividing the molecular weight of the assembly (185 kDa) by that of peptide **1** (2928 Da), giving 63.1, which is close to the ideal aggregation number (60) for dodecahedral assembly of *β*-annulus peptide.

In further experiments, we examined encapsulation of hexahistidine-tagged enhanced green fluorescent protein (His-tagged EGFP) into artificial viral capsids that were self-assembled from peptide **1** using SEC. It is known that dissociation constant of complex between Ni-NTA and hexahistidine-tag is about 10^{-8} M.[16] Briefly, aqueous solutions of His-tagged EGFP in Tris- HCl buffer were added to powdered

samples of peptide **1** to encapsulate EGFP within artificial viral capsids via the interaction between the His-tag and Ni-NTA. SEC of His-tagged EGFP alone showed one peak at 9.02 min (Figure 4b), whereas SEC of equimolar mixtures of His-tagged EGFP and the peptide **1** assembly showed two elution peaks at 7.02 and 9.62 min (Figure 4c), reflecting 91% encapsulation of EGFP in the artificial viral capsids and 9% free EGFP, respectively. Since isoelectric point (pI) of EGFP is 5.6, His-tagged EGFP possesses anionic charges on the surface. It is presumed that His- tagged EGFP was encapsulated into the peptide **1** assembly by not only specific interaction between His-tag and Ni-NTA, but also electrostatic interactions between anionic EGFP and cationic residues of artificial viral capsid. In contrast, SEC of equimolar mixtures of His-tagged EGFP and the unmodified β-annulus peptide **3** assembly showed that 91% of EGFP remained free, and only 9% of EGFP was non-specifically bound to the assembly (Figure 4d). The nonspecific binding will be caused by electrostatic interactions between EGFP and artificial viral capsid.

In further DLS experiments, equimolar mixtures of His-tagged EGFP and peptide **1** capsids had average diameters of 50.0 ± 17.5 nm, suggesting that encapsulation of EGFP had only minimal effects on the size distribution (Figure 5). A circular dichroism (CD) spectrum of the peptide **1** assembly showed negative peaks at 198 nm and 290 nm (Figure 6, blue). Conversely, a CD spectrum of the peptide **1** in the presence of equimolar His-tagged EGFP showed negative peaks at 215 nm and 290 nm, and the spectrum is almost consistent with the superposition of CD spectra for the peptide **1** assembly and EGFP (Figure 6, red). These results indicate that most His-tagged EGFP was encapsulated into Ni-NTA-modified artificial viral capsids with little change in size and conformation. Figure 7 shows the effect of concentration of His-tagged EGFP on the encapsulation into Ni-NTA-modified artificial viral capsids at [peptide **1**] = 0.1 mM. His-tagged EGFP at 0.01 mM were hardly encapsulated into capsids, and the concentration dependence gave sigmoidal curve which became saturated at 0.1-0.15 mM (almost 1:1 ratio). In contrast, His-tagged EGFP were minimally bound to the unmodified β-annulus peptide **3** (Figure 7, blue). These indicate that His-tagged EGFP would be cooperatively bound to Ni-NTA-modified artificial viral capsid without significant nonspecific binding.

Conclusions

We demonstrated that following N-terminal Ni-NTA modification, β-annulus peptides self-assembled into relatively stable artificial viral capsids of approximately 40 nm in size. Moreover, the present SEC analyses indicate that these artificial viral capsids efficiently encapsulate His-tagged EGFP. These data warrant further investigations on the controlled release of His-tagged EGFP, other protein drugs and enzymes in artificial viral capsids, which would provide novel platform for designing drug carriers and nano-reactors.

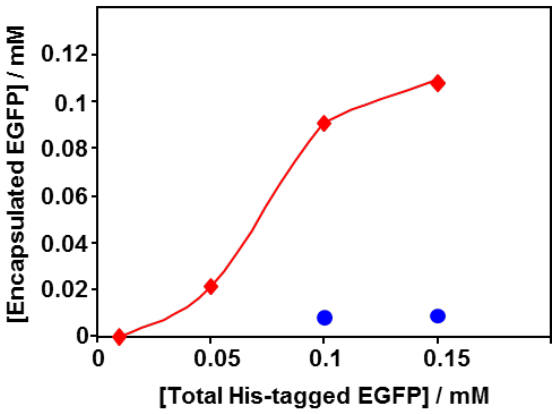

Fig. 7 The effect of concentration of His-tagged EGFP on the encapsulation into Ni-NTA-modified (red) and unmodified (blue) artificial viral capsids at [peptide] = 0.1 mM in 10 mM Tris-HCl buffer (pH 7.3) at 25°C.

Experimental section

General

Reagents were obtained from commercial sources and were used without further purification. Deionised water of high resistivity (>18 MΩ cm) was purified using a Millipore Purification System (Milli-Q water) and was used as a solvent for the present peptides. Reversed-phase HPLC was performed at ambient temperature using a Simadzu LC-6AD liquid chromatograph equipped with a UV/Vis detector (220 nm, Shimadzu SPD-10AVvp) and Inertsil ODS-3 (GL Science) columns (250 × 4.6 mm or 250 × 20 mm). MALDI-TOF mass spectra were obtained using an Autoflex III instrument (Bruker Daltonics) in linear/positive mode with α-cyano-4-hydroxy cinnamic acid (α-CHCA) as a matrix. CD spectra were taken at 25°C in a 1.0-mm quartz cell using a JASCO J-820 spectrophotometer equipped with a Peltier-type thermostatic cell holder. Laser Raman spectrometry in the solid state was performed using a JASCO NRS-3000 instrument. Recombinant enhanced green fluorescent protein with N-terminal His × 6 tags (His-tagged EGFP, MW = 27 kDa) was expressed in an Escherichia coli expression system, was purified using Ni-NTA resin and was confirmed using SDS-PAGE. Sequences of N-terminal His-tagged EGFP are shown in Figure 8.

MHHHHHHMVS KGEELFTGVVP ILVELDGDVN GHKFSVSGEG
EGDATYGKLT LKFICTTGKL PVPWPTLVTT LTYGVQCFSR
YPDHMKQHDF FKSAMPEGYV QERTIFFKDD GNYKTRAEVK
FEGDTLVNRI ELKGIDFKED GNILGHKLEY NYNSHNVYIM
ADKQKNGIKV NFKIRHNIED GSVQLADHYQ QNTPIGDGPV
LLPDNHYLST QSALSKDPNE KRDHMVLLEF VTAAGITLGM
DELY

Fig. 8 Sequence of His-tagged EGFP.

Synthesis of Cys-β-annulus peptide (2).

The peptide H-Cys(Trt)-Ile-Asn(Trt)-His(Trt)-Val-Gly-Gly-Thr(tBu)-Ile-Met-Ala-Pro-Val-Ala-Val-Thr(tBu)-Arg(Mtr)-Gln (Trt)-Leu-Val-Gly-Ser(tBu)-Alko-PEG resin was synthesised on Fmoc-Ser(tBu)-Alko-PEG resin (476 mg, 0.21 mmol/g; Watanabe Chemical Ind. Ltd) using standard Fmoc-based FastMoc coupling chemistry (5 eq. Fmoc-amino acids) with an ABI 433A synthesizer (Applied Biosystems). A dimethylformamide solution containing 2-(1H-benzotriazole-1-yl)-1, 1, 3, 3-tetramethyluronium hexafluorophosphate (HBTU, 0.5 M) and 1-hydroxybenzotriazole hydrate (HOBt•H2O, 0.5 M) was used as a coupling reagent. Neutralization and Fmoc deprotection was achieved using 2.0-M diisopropylamine in NMP and 20% piperidine in N-methylpyrrolidone (NMP), respectively. Peptidyl-resins were washed with NMP and were then dried under a vacuum. Peptides were deprotected and cleaved from the resin by treatment with a cocktail of trifluoroacetic acid (TFA)/1, 2-ethanedithiol/triisopropylsilane /water = 9.4/2.5/2.5/1.0 (mL) at room temperature for 3 h. Reaction mixtures were filtered to remove resins, and filtrates were concentrated under a vacuum. Peptides were precipitated by adding ice-cooled methyl-tert-butyl ether (MTBE) to the residue, and supernatants were decanted. After washing five times with MTBE, precipitated peptides were dried under vacuum. Crude products were purified using reversed-phase HPLC (Inertsil ODS-3) and were eluted with a linear gradient of CH3CN/water (25/75 to 27/73 over 100 min) containing 0.1% TFA. Eluted fractions containing desired peptides were lyophilised to give flocculent solids. The isolated yield was 32 mg (14%); MALDI-TOF-MS (matrix: α-CHCA): m/z = 2408.0 ($[M + H]^+$).

Preparation of Ni-NTA-modified-β-annulus peptide (1).

Cys-β-annulus peptide **2** in 0.5 mL of 0.5-mM aqueous solution was degassed by N2 bubbling and was mixed with 0.5 mL of a 1.0-mM aqueous solution (degassed by N_2 bubbling) of maleimido-C_3-NTA (Dojindo Laboratories) at room temperature. After incubating for 12 h at room temperature, mixtures were purified using reversed-phase HPLC (Inertsil ODS-3) and were eluted with a linear gradient of acetonitrile/water (25/75 to 27/73 over 100 min) containing 0.1% TFA to provide pure NTA-β-annulus peptide (isolated yield: 0.74 mg, 52%); MALDI-TOF-MS (matrix: α-CHCA): m/z = 2835.1 ($[M + H]^+$).

NTA-β-annulus peptide (3.2 mg) were dissolved in 10-mM Tris-HCl buffer to prepare 5.6-mM aqueous solutions. Subsequently, 50-mM aliquots of $NiCl_2$ solution in 10-mM Tris-HCl buffer were added to peptide solutions to [peptide] and [Ni^{2+}] of 5.0 mM. Ni-complex **1** formation was confirmed using MALDI-TOF-MS (matrix: α-CHCA): m/z = 2892.3 ($[M + H]^+$).

Dynamic Light Scattering.

Stock solutions (1.0 mM) of Ni-NTA-β-annulus peptide **1** in 10-mM Tris-HCl buffer were prepared by dissolving in buffer without sonication or heating. Samples were prepared by diluting stock solutions with 10-mM Tris-HCl buffer and were incubated at 25°C for 12 h before DLS measurements using a Zetasizer Nano ZS (MALVERN) instrument at 25°C with an incident He–Ne laser (633 nm). During measurements, count rates (sample scattering intensities) were also provided. Correlation times of scattered light intensities $G(\tau)$ were measured several times and means were calculated and fitted to equation 1, where B is baseline, A is amplitude, q is scattering vector, τ is delay time and D is the diffusion coefficient.

$$G(\tau) = B + A \exp(-2q^2 D\tau) \quad (1)$$

Hydrodynamic radii (RH) of scattering particles were calculated using the Stokes–Einstein equation (eq. 2), where η is solvent viscosity, k_B is Boltzmann's constant and T denotes the absolute temperature.

$$R_H = k_B T/6\pi\eta D \quad (2)$$

Scanning Electron Microscopy.

DLS samples were observed using SEM. Briefly, 5 μL aliquots of DLS samples were applied to hydrophilised carbon-coated Cu-grids (ALLANCE Biosystems) for 60 s and were then removed. Grids were then dried in vacuo, coated with platinum (ca. 3 nm, Hitachi E-1030 ion sputter) and then observed using SEM (Hitachi S-5000) with an acceleration voltage of 15 kV at a tilt angle of 30°.

Transmission Electron Microscopy.

5 μL aliquots of DLS samples were applied to hydrophilised carbon-coated Cu-grids (ALLANCE Biosystems) for 60 s and were then removed. A drop of 2 wt% aqueous sodium phosphotungstate was placed on each of the grids. After the sample-loaded carbon-coated grids were dried in vacuo, they were observed by TEM (JEOL JEM 1400 Plus) using an acceleration voltage of 80 kV.

Size Exclusion Chromatography.

SEC analyses of the assemblies of Ni-NTA-modified β-annulus peptide **1** (0.1 mM), His-tagged EGFP (0.1 mM) and their equimolar mixture after elution with 10 mM Tris-HCl buffer (pH 7.3) were performed at 25°C using a Shimadzu LC-6AD liquid chromatograph equipped with a UV/Vis detector (Shimadzu SPD-10AVvp) and a TSKgel G3000SWXL (TOSOH Bioscience, 300 × 7.8 mm ID). SEC of peptide 1 was monitored at 220 nm, whereas those of His-tagged EGFP and the mixture were monitored at 488 nm. Calibration curve (Figure 7) was prepared using thyroglobulin (669 kDa), γ-globulin (160 kDa), ribonuclease A (137 kDa) and p-aminobenzoic acid (137 Da) as molecular weight standards. Nonlinear curve fitting of calibration curve indicated that the relationship between the logarithm of molecular weight and elution volume (x/mL) could be expressed as follows:

$$\log M_n = 0.0022x^3 - 0.0702x^2 + 0.2588x + 6.1545 \quad (3)$$

Apparent average molecular weights of assemblies of Ni-NTA-modified β-annulus peptide 1 were estimated from calibration curve using equation 3.

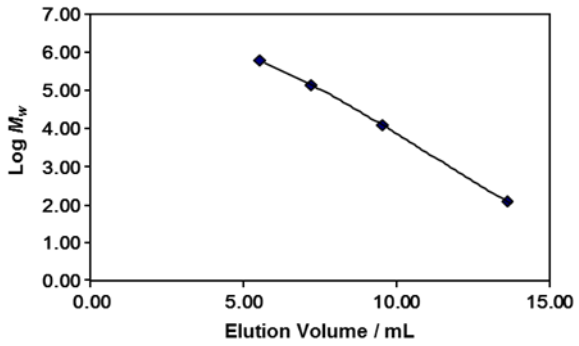

Fig.9 Calibration curve for SEC analyses; Thyroglobulin (669 kDa), γ-globulin (160 kDa), ribonuclease A (137 kDa) and p-aminobenzoic acid (137 Da) were used as molecular weight standards.

Acknowledgements

This research was partially supported by The Mitsubishi Foundation and a Grant-in-Aid for Scientific Research (B) (No. 15H03838) from the Japan Society for the Promotion of Science (JSPS).

Notes and references

1 For reviews: (a) T. Douglas and M. Young, *Science*, 2006, **312**, 873; (b) N. F. Steinmetz and D. J. Evans, *Org. Biomol. Chem.*, 2007, **5**, 2891; (c) D. Parapostolou and S. Howorka, *Mol. Biosyst.*, 2009, **5**, 723; (d) L. S. Witus and M. B. Francis, *Acc. Chem. Res.*, 2011, **44**, 774; (e) L. M. Bronstein, *Small*, 2011, **7**, 1609.

2 (a) M. Comellas-Aragonès, H. Engelkamp, V. I. Claessen, N. A. J. M. Sommerdijik, A. E. Rowan, P. C. M. Christianen, J. C. Maan, B. J. M. Verduin, J. J. L. M. Cornelissen, and R. J. M. Nolte, *Nature Nanotech.*, 2007, **2**, 635; (b) I. J. Minten, L. J. A. Hendriks, R. J. M. Nolte, and J. J. L. M. Cornelissen, *J. Am. Chem. Soc.*, 2009, **131**, 17771.

3 J. D. Fiedler, S. D. Brown, J. L. Lau, and M. G. Finn *Angew. Chem. Int. Ed.*, 2010, **49**, 9648.

4 (a) F. P. Seebeck, K. J. Woycechowsky, W. Zhuang, J. P. Rabe, and D. Hilvert, *J. Am. Chem. Soc.*, 2006, **128**, 4516; (b) B. Wörsdörfer, Z. Pianowski, and D. Hilvert, *J. Am. Chem. Soc.*, 2012, **134**, 909; (c) Y. Azuma, R. Zschoche, M. Tinzl, and D. Hilvert, *Angew. Chem. Int. Ed.*, 2016, **55**, 1531.

5 For reviews: (a) K. Matsuurua, *RSC Adv.*, 2014, **4**, 2942; (b) B. E. I. Ramakers, J. C. M. van Hesta, and D. W. P. M. Löwik, *Chem. Soc. Rev.*, 2014, **43**, 2743; (c) E. D. Santis, M. G. Ryadnov, *Chem. Soc. Rev.*, 2015, **44**, 8289.

6 (a) J. C. T. Carlson, S. S. Jena, M. Flenniken, T. F. Chou, R. A. Siegel, and C. R. Wagner, *J. Am. Chem. Soc.*, 2006, **128**, 7630; (b) H. Kitagishi, K. Oohora, H. Yamaguchi, H. Sato, T. Matsuo, A. Harada, and T. Hayashi, *J. Am. Chem. Soc.*, 2007, **129**, 10326.

7 (a) J. E. Padilla, C. Colovos, and T. O. Yeates, *Proc. Nat. Acad. Sci., USA*, 2001, **98**, 2217; (b) Y. T. Lai, D. Cascio, and T. O. Yeates, *Science*, 2012, **336**, 1129; (c) Y. T. Lai, K. L. Tsai, M. R. Sawaya, F. J. Asturias, and T. O. Yeates, *J. Am. Chem. Soc.*, 2013, **135**, 7738; (d) Y. T. Lai, E. Reading, G. L. Hura, K.-L. Tsai, A. Laganowsky, F. J. Asturias, J. A. Tainer, C. V. Robinson, and T. O. Yeates, *Nat. Chem.*, 2014, **6**, 1065.

8 J. M. Fletcher, R. L. Harniman, Fr. R. H. Barnes, A. L. Boyle, A. Collins, J. Mantell, T. H. Sharp, M. Antognozzi, P. J. Booth, N. Linden, M. J. Miles, R. B. Sessions, P. Verkade, and D. N. Woolfson, *Science,* 2013, **340**, 595.

9 H. Gradišar, S. Božič, T. Doles, D. Vengust, I. Hafner-Bratkovič, A. Mertelj, B. Webb, A. Šali, S. Klavžar, and R. Jerala, *Nat. Chem. Biol.*, 2013, **9**, 362.

10 (a) H. Zhang, J. Fei, X. Yan, A. Wang, and J. Li, *Adv. Funct. Mater.* 2015, **25**, 1193; (b) R. Xing, K. Liu, T. Jiao , N. Zhang, K. Ma, R. Zhang, Q. Zou, G. Ma, and X. Yan, *Adv. Mater.* 2016, **28**, 3669; (c) K. Liu, R. Xing, Q. Zou, G. Ma, H. Möhwald, X. Yan, *Angew. Chem. Int. Ed.*, 2016, **55**, 3036.

11 K. Matsuura, *Polymer J.*, 2012, **44**, 469.

12 (a) K. Matsuura, K. Murasato, and N. Kimizuka, *J. Am. Chem. Soc.*, 2005, **127**, 10148; (b) K. Murasato, K. Matsuura, and N. Kimizuka, *Biomactromolecules*, 2008, **9**, 913; (c) K. Matsuura, H. Hayashi, K. Murasato, and N. Kimizuka, *Chem. Commun.*, 2011, **47**, 265; (d) K. Matsuura, K. Murasato, and N. Kimizuka *Int. J. Mol. Sci.*, 2011, **12**, 5187.

13 (a) K. Matsuura, H. Matsuyama, T. Fukuda, T. Teramoto, K. Watanabe, K. Murasato, and N. Kimizuka, *Soft Matter*, 2009, **5**, 2463; (b) K. Matsuura, K. Fujino, T. Teramoto, K. Murasato, and N. Kimizuka *Bull. Chem. Soc. Jpn.*, 2010, **83**, 880; (c) K. Matsuura, K. Tochio, K. Watanabe, and N. Kimizuka *Chem. Lett.*, 2011, **40**, 711.

14 (a) K. Matsuura, K. Watanabe, K. Sakurai, T. Matsuzaki, and N. Kimizuka, *Angew. Chem. Int. Ed.*, 2010, **49**, 9662; (b) K. Matsuura, K. Watanabe, Y. Matsushita, and N. Kimizuka, *Polymer J.*, 2013, **45**, 529; (c) S. Fujita and K. Matsuura, *Nanomaterials,* 2014, **4**, 778; (d) K. Matsuura, G. Ueno, and S. Fujita, *Polymer J.*, 2015, **47**, 146; (e) K. Matsuura, Y. Mizuguchi, and N. Kimizuka, *Biopolymers (Pept. Sci.)*, 2016, DOI: 10.1002/bip.22774. (f) S. Fujita and K. Matsuura, *Chem. Lett.*, 2016, DOI: 10.1246/cl.160396.

15 T. Miura, T. Satoh, I. A. Hori, H. Takeuchi, *J. Raman Spectrosc.*, 1998, **29**, 41.

16 S. Knecht, D. Ricklin, A. N. Eberle, B. Ernst, *J. Mol. Recognit.,* 2009, **22**, 270.